Wearable Multiple Body Signal Monitoring System with Single Biocompatible AlN Piezoelectric Sensor

Wearable Multiple Body Signal Monitoring System with Single Biocompatible AlN Piezoelectric Sensor

Suleyman Mahircan Demir*†§, Lorenzo Marzano*‡§, Paolo Motto Ros†, Luca Fachechi§, Danilo Demarchi† and Massimo De Vittorio‡§
Email: {suleyman.demir,paolo.mottoros,danilo.demarchi}@polito.it {lorenzo.marzano,luca.fachechi,massimo.devittorio}@iit.it
†Department of Electronics and Telecommunications, Politecnico di Torino, Turin, Italy
‡Department of Engineering and Innovation, Università del Salento, Lecce, Italy
§ Center for Biomolecular Nanotechnologies, Istituto Italiano di Tecnologia, Arnesano (LE), Italy

***Abstract*— Remote monitoring of vital body signals has drawn the attention of late, particularly with the burst of COVID-19. Wearable devices are started to be widely used for non-invasive health monitoring tasks. This work presents a wearable system for multiple body signal monitoring using only one biocompatible aluminum nitride piezoelectric sensor and a custom wireless electronic device for data acquisition and transmission. The proposed sensor has been customized for the suprasternal notch, where we can simultaneously extract heart rate, respiration rate, and deglutition events. These parameters are helpful for the remote diagnosis of multiple diseases like cardiac arrhythmia, asthma, and dysphagia. Moreover, heart sound components have been derived from the same signal, providing critical information about heart health and insight into possible heart diseases. The preliminary experimental results show that the proposed wearable system can be used for personalized healthcare applications and offers a promising solution for unobtrusive remote health monitoring.**

Keywords—wearable devices, piezoelectric sensor, aluminum nitride, remote health monitoring, heart sound, heart rate, respiration, deglutition

I. Introduction

Continuous developments in sensor technologies, together with the advantage of small-footprint electronics and the advancement of machine learning, pave the way for the daily utilization of wearable sensors and devices in various applications. Employing these ubiquitous devices for remote monitoring of physiological parameters has gained importance. Considering the provided advantages such as early disease diagnosis, reduction in health expenses, and comfort for daily utilization, the wearable sensors market value is projected to be $5.76 Bn by 2028, whereas it was $1.90 Bn in 2021 [1].

Particularly, with the breaking out of the COVID-19 emergency, wearables have attracted the attention of academia and industry. For instance, the correlation between the early symptoms of COVID-19 and some physiological parameters (heart rate, respiration rate, and skin temperature) recognizable by wearable devices has been systematically reviewed by Miratza et al. [2] to reveal the potential of wearable sensors for the early diagnosis of the COVID-19 infection. The potential of wearables is not only limited to COVID-19 diagnosis. Latterly, researchers have been exploring wearable technologies and developing wearable sensors and systems to acquire various biosignals for diagnosing sundry diseases such as cardiac arrhythmia, breast cancer, glaucoma, dysphagia, respiration disorders, mental stress, etc. [3-8].

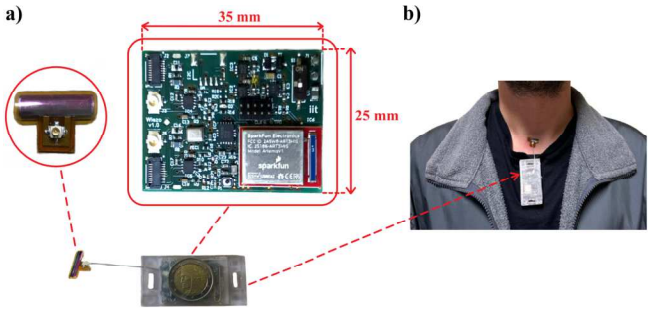

Fig. 1. Proposed wearable device depiction (a) system components (b) device on a volunteer subject.

Recent studies focus profoundly on piezoelectric sensors for monitoring body signals as they can provide multiple pieces of information by converting mechanical movement into an electrical signal. For example, a phonocardiogram (PCG) signal is an important physiological parameter for identifying heart murmurs, which can help to diagnose different heart diseases [9]. Using a chest belt, the authors in [10] use a commercial PVDF piezo film sensor to record heart sounds and respiration-related thorax motion. However, PVDF-based sensors face some difficulties when placed in moving parts of the body due to low adhesion to the skin. Moreover, trying to limit this effect confronts technological issues such as degradation in piezoelectricity, as reported in [11]. Another work presented in [12] proposes a system for the outer chest surface to observe respiration and cardiac activities. Nonetheless, a large and thick lead-zirconate-titanate (PZT) film is used as a sensor, making the system bulky. Mengjiao Qu et al. [13] utilize an aluminum nitride (AlN) based piezoelectric MEMS acoustic sensor to record PCG and detect swallowing movement. Similarly, Natta et al. [11] use an AlN piezoelectric sensor for dysphagia diagnosis by placing the sensor on laryngeal prominence. Biocompatibility and non-toxicity make this material the optimal piezoelectric sensor choice for biomedical applications and wearable systems [14]. Moreover, the quality of the film and the sensor shape can be easily adapted for different applications. Nevertheless, the authors in [13] utilize an array of sensors in different positions (chest and neck) to detect heart sounds and swallowing separately. Furthermore, the proposed wired system may create discomfort in daily usage. On the other hand, only deglutition events have been targeted in [11] for dysphagia diagnosis by using a large data acquisition system. Thus, there is still room for developing a compact wireless wearable system using an AlN piezoelectric sensor for unobtrusive monitoring of multiple physiological parameters, ideally from a single body location.

* S.M. Demir and L. Marzano contributed equally to this work.

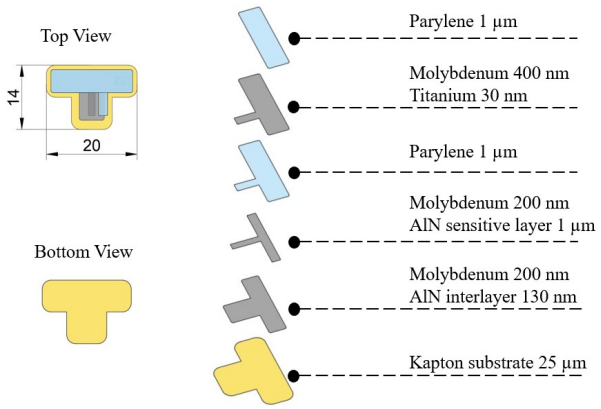

Fig. 2. Proposed AlN piezoelectric sensor and breakdown of its layers.

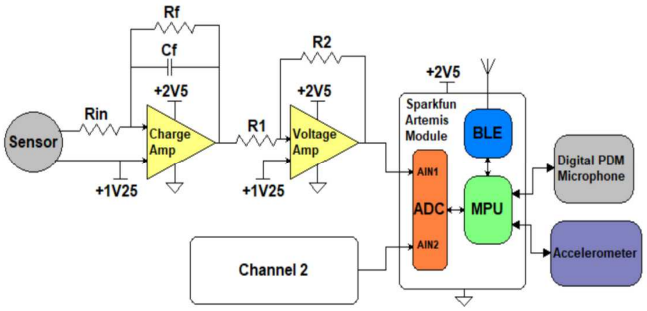

Fig. 3. Simplified schematic of the custom PCB showing the details of one channel to visualize data acquisition and transmission stages.

In this work, we propose a wearable multiple body signal monitoring system employing a single biocompatible AlN piezoelectric sensor. The complete system is depicted in Fig. 1 (a). The wearable sensor structure is similar to the smart patch presented in [11]. Yet, the sensor shape is here optimized for the suprasternal notch (SSN) for non-invasive and unobtrusive monitoring. The main reason for tailoring the sensor for the SSN is that this particular position provides four different body signals: heart sound, heart rate, respiration rate, and deglutition events. This makes the SSN unique for the proposed AlN sensor. Furthermore, the sensor customization also contributes to the user's comfort thanks to the elongated shape fitting the SSN. In addition, a custom PCB has been specifically designed for this work to perform data acquisition and wireless data transmission. For the preliminary experiments, a simple case has been printed for developing a comfortable wearable device.

The rest of the paper is organized as follows: the wearable system components, encompassing the AlN sensor and the custom electronics, are introduced in Section II. The experimental results are presented and discussed in detail in Section III. Lastly, in Section IV, the conclusion and future perspectives are debated.

II. System Design

A. AlN Piezoelectric Sensor

The piezoelectric sensor, shown in Fig. 1 (a), is based on AlN with the structure grown on a Kapton foil; this results in a biocompatible and flexible sensor that follows the geometry of the SSN. The microfabrication techniques followed for realizing this sensor make the sensor shape modification easier. This fabrication flexibility allows for the sensor's reshaping depending on the application. In this case, a rectangular and elongated form is chosen to fit the SSN. The sensor has an active area of 30 mm^2 with a maximum dimension of 20 mm by 14 mm. The sensor multilayer stack is delineated in Fig. 2 and fabricated by following the lithography steps for the patterning of the different layers obtained through sputtering deposition, while the protective parylene layers are deposited with a parylene coater and patterned with plasma oxygen. All the fabrication steps are carried out with the substrate attached to a silicon wafer using polydimethylsiloxane (PDMS), so after the whole fabrication process, a laser cutting machine is used to shape the substrate around the single sensor to detach it from the wafer. The electrical characterization is performed using an LCR meter. The parallel capacitance and the parallel resistance have been measured as 3.39 nF and 3.65 MΩ, respectively.

B. Custom PCB and Case Design

The main design requirements of the electronics for the data acquisition and wireless data transmission were:

- Convert the charge output of the sensor into a voltage with high signal-to-noise (SNR) ratio.
- Avoid filtering vital information.
- Amplify the signal when input is meager.
- Transmit the data with low power consumption to prolong the battery life.
- Reduce the footprint for unobtrusive monitoring.

Considering all these aspects, a 4-layer PCB has been designed and manufactured. The simplified schematic of one channel (each actual PCB has two identical channels) is presented in Fig. 3 to visualize the data acquisition and transmission stages. The gain of the charge amplifier is set to 1 mV/pC to accomplish a balanced gain and SNR. A large feedback resistor (R_f) is used in this stage to reduce high pass filtering as the respiration signal frequency is between 0.2-0.3 Hz [15]. Also, a series resistor, R_{in}, is added to the inverting input terminal to enhance stability and limit the input current due to unexpected excessive input voltage [16]. A voltage gain stage is utilized as the second stage to amplify further the converted voltage by setting the R_2/R_1 ratio.

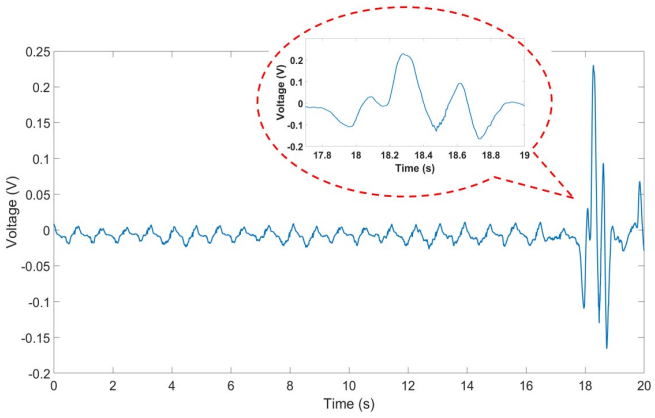

Fig. 4. Recorded signal with deglutition event from the SSN.

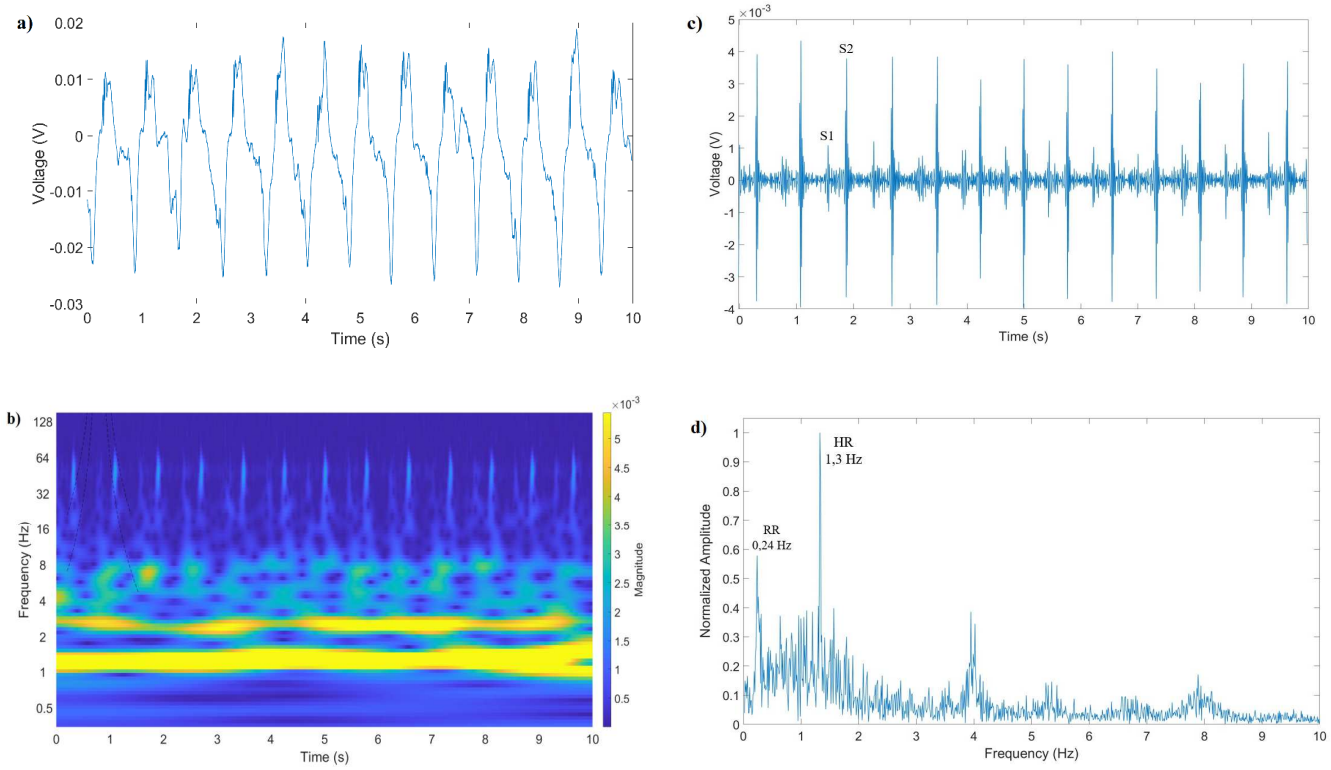

Fig. 5. Analysis of the recorded signal (a) the first 10 seconds of the signal to eliminate the deglutition event (b) spectrogram of the new signal (c) the new signal filtered to demonstrate heart sound components S1 and S2 (d) normalized FFT of the new signal.

Furthermore, the Sparkfun Artemis Module [17] (enclosing an Ambiq Apollo 3 Blue processor) is integrated into the system to perform ADC and BLE communication. Ambiq Apollo 3 Blue has an active current consumption of 6 µA/MHz, which provides low power consumption, thus prolonging the battery life. Moreover, a reverse current protection circuit has been incorporated into the PCB for safety, with a 3-axis accelerometer and a pulse density modulation (PDM) microphone for future applications. In the end, the overall PCB dimension is 25 mm by 35 mm. The PCB is powered by a standard 3.7 V 250 mAh rechargeable lithium polymer (Li-Po) battery [18], and a simple case (60 mm × 30 mm × 15 mm) has been designed and printed using a 3D printer (Asiga Pico) to develop a wearable device. The final PCB (named Wiezo) is depicted alongside the AlN sensor and the entire system in Fig. 1 (a).

III. Experimental Results and Discussion

The signal in Fig. 4 has been acquired with a 1 kHz sampling rate and 10 mV/pC overall gain by placing the sensor on the SSN, shown in Fig. 1 (b), while the subject was resting for 20 seconds. Moreover, a deglutition event occurs between the 17th and 19th seconds. The preliminary analysis confirmed that the obtained results are in line with the results reported in [11] for swallowing disorder assessment, while the size of the electronics is five times smaller in volume. Besides, the average current consumption of 2.95 mA has been measured during the amplification, ADC, and BLE continuous data transfer, leading to the average power consumption of 10.9 mW. Hence, the device is expected to be uninterruptedly working for more than 84 hours, 3.5 days, using the aforementioned Li-Po battery [18].

In addition, relocating the sensor from laryngeal prominence, as in [11], to the SSN allows for the extraction of heart sound components. Although these heart sounds cannot be easily recognized in the waveform, the signal is processed to highlight these components. In Fig. 5 (a), the first 10 seconds of the signal depicted in Fig. 4 is provided to eliminate the deglutition event and smoothly demonstrate the rest of the signal. The scalogram shown in Fig. 5 (b) represents the magnitude of the continuous wavelet transform (CWT) of the signal in Fig. 5 (a). In this graph, plotting the signal as a function of time and frequency, the peaks regarding the two heart sounds, S1 and S2, are clear and identified by the peaks reaching approximately a maximum frequency of 80 Hz. In [19], S1 frequency is provided between 25-45 Hz, while S2 frequency is reported as 50 Hz for a healthy person. The heart sound frequency spectrum is also concentrated within the 20-150 Hz range for a healthy heart [20]. These frequencies may vary with the presence of a heart problem. However, in this work, our preliminary findings for the frequency distribution of heart sounds align with the results presented in [19] and [20] by considering that the volunteered subject is healthy.

Moreover, the signal in Fig. 5 (a) has been software filtered (1st order high pass filter with 30 Hz cutoff frequency) to emphasize the heart sound components S1 and S2. The resulting waveform is presented in Fig. 5 (c). The lower peak-to-peak represents S1, and the higher one represents S2. The differences in loudness could explain the amplitude difference between these two components. S2 is louder compared to S1 in the base of the heart, whereas S1 is louder in the apex of the heart [21]. Since the sensor was situated on the SSN, which is closer to the base of the heart, the S2 amplitude is higher than the S1. Also, the heart sound

components can be correlated with an ECG waveform. Occurrences of S1 components are correlated with the R waves of an ECG signal, whereas occurrences of S2 components are correlated with the endpoint of the T waves [22]. Furthermore, the time between the starting point of S1 and S2 belongs to the systolic duration, and the time between the starting point of S2 and the next S1 belongs to the diastolic duration. These durations are valuable for recognizing emotions and providing insights into mental health, such as depression, anxiety, stress level, etc., thanks to the possibility of extracting the heart rate variability (HRV) parameter [23, 24]. Unambiguous identification of heart sound components could also be a crucial factor for the early diagnosis of heart diseases since observing some heart murmurs could imply abnormalities like valve damage or improper closure of valves [9, 22]. The proposed wireless wearable system demonstrates an encouraging performance on the volunteer for non-invasive heart sound monitoring while simultaneously acquiring respiration rate (RR), heart rate (HR), and deglutition events.

Locating the sensor on the SSN also allows the detection of low-frequency components revealing the RR and HR. In Fig. 5 (d), the signal's normalized Fast Fourier Transform (FFT) is depicted. Looking at the FFT, the RR, and HR can be noticed. The first two frequency peaks observed at 0.24 Hz and 1.3 Hz belong to RR and HR, respectively. The RR was expected to be around 0.2-0.3 Hz, as reported by [15], and found in this range while resting. During the experiment, OMRON M3 Comfort (HEM-7154-E) Blood Pressure Monitor [25], clinically validated, was used simultaneously to validate HR. The blood pressure monitor reported the HR as 78 beats per minute (bpm), the same as our finding (1.3 Hz is equal to the heart rate of 78 bpm).

IV. Conclusion and Future Perspectives

The experimental results demonstrate that the proposed wireless wearable device can successfully identify heart sound components (S1 and S2), respiration rate, heart rate, and deglutition events from the SSN by employing only one AlN piezoelectric sensor. In addition, we can take advantage of the AlN sensor scalability and modify the sensor shape for a particular person to develop a customized wearable device that contributes to personalized healthcare studies. Moreover, by employing this system, it is possible to extract heart rate variability, which may indicate physical heart conditions and mental health conditions such as depression, anxiety, stress level, etc. Besides, it may help to diagnose respiration disorders, dysphagia, cardiac arrhythmia, and heart-related diseases early. The possibility of the remote and early diagnosis of multiple diseases with only one sensor would be pleasant for individuals while reducing the workload of healthcare personnel.

The next step is to perform clinical tests and analyze the findings in-depth to improve the system. Furthermore, we consider sensor-fabric integration and flexible electronic production for developing an intelligent textile product. Also, as the AlN piezoelectric sensor shows mechano-acoustic behavior, the speech and voice detection possibility will be examined in detail while we keep monitoring the signals presented in this work. Lastly, the case size and design will be further optimized for the user's comfort and daily usage according to the feedback from clinical tests.

References

[1] The Insight Partners, “Wearable Sensors Market Size hit US$ 5,762.57 million by 2028,” theinsightpartnerts.com. https://www.theinsightpartners.com/pr/wearable-sensors-market (accessed Oct. 20, 2022).

[2] M. Mitratza *et al.*, “The performance of wearable sensors in the detection of SARS-CoV-2 infection: a systematic review,” *The Lancet Digital Health*, vol. 4, no. 5, pp. e370–e383, May 2022, doi: 10.1016/s2589-7500(22)00019-x.

[3] S. S. Gambhir, T. J. Ge, O. Vermesh, and R. Spitler, “Toward achieving precision health,” *Science Translational Medicine*, vol. 10, no. 430, Feb. 2018, doi: 10.1126/scitranslmed.aao3612.

[4] S. S. Gambhir, T. J. Ge, O. Vermesh, R. Spitler, and G. E. Gold, “Continuous health monitoring: An opportunity for precision health,” *Science Translational Medicine*, vol. 13, no. 597, Jun. 2021, doi: 10.1126/scitranslmed.abe5383.

[5] H. Zhang *et al.*, “Graphene-enabled wearable sensors for healthcare monitoring,” *Biosensors and Bioelectronics*, vol. 197, p. 113777, Feb. 2022, doi: 10.1016/j.bios.2021.113777.

[6] B. Polat *et al.*, “Epidermal Graphene Sensors and Machine Learning for Estimating Swallowed Volume,” *ACS Applied Nano Materials*, vol. 4, no. 8, pp. 8126–8134, Aug. 2021, doi: 10.1021/acsanm.1c01378.

[7] A. Natarajan *et al.*, “Measurement of respiratory rate using wearable devices and applications to COVID-19 detection,” *npj Digital Medicine*, vol. 4, no. 1, Sep. 2021, doi: 10.1038/s41746-021-00493-6.

[8] H. Miwa and K. Sakai, "Development of heart rate and respiration rate measurement system using body-sound," *2009 9th International Conference on Information Technology and Applications in Biomedicine*, 2009, pp. 1-4, doi: 10.1109/ITAB.2009.5394438.

[9] Y. Zeinali and S. T. A. Niaki, “Heart sound classification using signal processing and machine learning algorithms,” *Machine Learning with Applications*, p. 100206, Nov. 2021, doi: 10.1016/j.mlwa.2021.100206.

[10] P. Bifulco *et al.*, "Monitoring of respiration, seismocardiogram and heart sounds by a PVDF piezo film sensor," *Measurement*, vol. II, p.786-789, 2014.

[11] L. Natta *et al.*, “Conformable AlN Piezoelectric Sensors as a Non-invasive Approach for Swallowing Disorder Assessment,” *ACS Sensors*, vol. 6, no. 5, pp. 1761–1769, May 2021, doi: 10.1021/acssensors.0c02339.

[12] A. Allataifeh and M. Al Ahmad, “Simultaneous piezoelectric non-invasive detection of multiple vital signs,” *Scientific Reports*, vol. 10, no. 1, Jan. 2020, doi: 10.1038/s41598-019-57326-6.

[13] M. Qu *et al.*, “Monitoring of physiological sounds with wearable device based on piezoelectric MEMS acoustic sensor,” *Journal of Micromechanics and Microengineering*, vol. 32, no. 1, p. 014001, Nov. 2021, doi: 10.1088/1361-6439/ac371e.

[14] A. Bongrain *et al.*, “A New Technology of Ultrathin AlN Piezoelectric Sensor for Pulse Wave Measurement,” *Procedia Engineering*, vol. 120, pp. 459–463, 2015, doi: 10.1016/j.proeng.2015.08.668.

[15] Cleveland Clinic, “Vital Signs,” my.clevelandclinic.org. Jan. 23, 2019. https://my.clevelandclinic.org/health/articles/10881-vital-signs (accessed Oct. 20, 2022).

[16] Analog Devices, “12-Bit, 1 MSPS, Single-Supply, Two-Chip Data Acquisition System for Piezoelectric Sensors,” AD, Norwood, MA, USA, Circuit Note CN-0350. Accessed: Oct. 20, 2022. [Online]. Available: https://www.analog.com/en/design-center/reference-designs/circuits-from-the-lab/CN0350.html?doc=CN0350.pdf#rd-overview

[17] Sparkfun Electronics, “SparkFun Artemis Module - Low Power Machine Learning BLE Cortex-M4F,” WRL-15484 documents. Accessed: Oct. 20, 2022. [Online]. Available: https://www.sparkfun.com/products/15484

[18] Cellevia Batteries, “Polymer Lithium-Ion Battery,” 502030 datasheet, Sep. 3, 2016. Accessed: Oct. 20, 2022. [Online]. Available: https://www.tme.eu/Document/6e40ea251c9a5e9afeb789fbbf73f3f5/cel0005.pdf

[19] K. Phua, J. Chen, T. H. Dat, and L. Shue, “Heart sound as a biometric,” *Pattern Recognition*, vol. 41, no. 3, pp. 906–919, Mar. 2008, doi: 10.1016/j.patcog.2007.07.018.

[20] F. Arvin, S. Doraisamy, and E. Safar Khorasani, “Frequency shifting approach towards textual transcription of heartbeat sounds,” *Biological Procedures Online*, vol. 13, no. 1, Oct. 2011, doi: 10.1186/1480-9222-13-7.

[21] Access Pharmacy from McGraw-Hill, “Cardiovascular: Auscultation: First and Second Heart Sounds,” accesspharmacy.mhmedical.com. https://accesspharmacy.mhmedical.com/data/interactiveguide/physexam/cardio/s1s2.html (accessed Oct. 20, 2022).

[22] M. B. Malarvili, I. Kamarulafizam, S. Hussain and D. Helmi, "Heart sound segmentation algorithm based on instantaneous energy of electrocardiogram," *Computers in Cardiology, 2003*, 2003, pp. 327-330, doi: 10.1109/CIC.2003.1291157.

[23] Harvard Health Publishing Staff, “Heart rate variability: A new way to track well-being,” health.harvard.edu. Dec. 1, 2021. https://www.health.harvard.edu/blog/heart-rate-variability-new-way-track-well-2017112212789 (accessed Oct. 20, 2022).

[24] C. Xiefeng, Y. Wang, S. Dai, P. Zhao, and Q. Liu, “Heart sound signals can be used for emotion recognition,” *Scientific Reports*, vol. 9, no. 1, p. 6486, Apr. 2019, doi: 10.1038/s41598-019-42826-2.

[25] Omron Healthcare, “M3 Comfort Upper Arm Blood Pressure Monitor,” HEM-7154-E specifications. Accessed: Oct. 20, 2022. [Online]. Available: https://www.omron-healthcare.com/eu/blood-pressure-monitors/m3_2.html